Inorganic Chemistry

ARTICLE

pubs.acs.org/IC

Heteroatomic Molecular Clusters Derived from Group 15 Zintl Ion Cages: Synthesis and Isolation of $[M_2(HP_7)_2]^{2-}$ (M = Ag, Au), Two Novel Cluster Anions Exhibiting Metallophilic Interactions

Caroline M. Knapp, Charlotte S. Jackson, Joseph S. Large, Amber L. Thompson, and Jose M. Goicoechea*

Department of Chemistry, Chemistry Research Laboratory, University of Oxford, Mansfield Road, Oxford OX1 3TA, U.K.

Supporting Information

ABSTRACT: Ethylenediamine (en) solutions of K_3P_7 and 2,2,2-crypt (4,7,13,16,21,24-hexaoxa-1,10-diazabicyclo[8.8.8] hexacosane) were reacted with the homoleptic group 11 complexes $[M(nbe)_3][SbF_6]$ (M = Ag, Au; nbe = norbornene) yielding two novel cluster anions, $[M_2(HP_7)_2]^{2-}$, both of which were isolated in low crystalline yields as $[K(2,2,2\text{-crypt})]_2[M_2(HP_7)_2]$ (M = Ag (**1**) and Au (**2**)). Optimization of the reaction conditions by incorporation of a proton source (ammonium tetraphenylborate) and the replacement of the light-sensitive nbe adducts of silver and gold with the chloride salts MCl (M = Ag, Au) was found to greatly increase the yield and purity in which **1** and **2** were isolated. Compounds **1** and **2** were characterized by single crystal X-ray diffraction, electrospray ionization mass-spectrometry (ESI− MS), elemental analysis, and ^1H and ^{31}P NMR spectroscopy. Density functional theory (DFT) calculations on the cluster anions were also conducted.

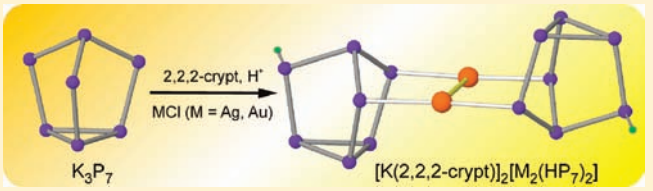

1. INTRODUCTION

In recent years great insight has been gained into the solution reactivity of "naked" Zintl cluster anions of the group 15 elements, particularly in the case of the heptapnictide trianions, $[E_7]^{3-}$ (E = P, As, Sb).[1] Dissolution of A_3E_7 alloys (A = alkali metal; E = P, As, Sb) in polar, nonprotic solvents (e.g., ethylenediamine or liquid ammonia) is known to yield solutions of $[E_7]^{3-}$ cages. Such species have nortricylane-like structures and according to the valence bond formalism are "electron-precise" clusters, where all of the E-E interactions may be considered as two-center, two-electron bonds. The negative charges of the cluster anions are formally localized on the two coordinate atoms. Numerous research groups have studied the behavior of these species in solution, in particular that of the heptaphosphide $[P_7]^{3-}$ cage, on account of the insights offered by ^{31}P NMR spectroscopy. Early studies by Baudler and co-workers used ^{31}P NMR spectroscopy to probe the fluxional nature of the $[P_7]^{3-}$ cluster in solution.[2] At room temperature the only observable feature in the ^{31}P NMR spectrum of $[P_7]^{3-}$ is a broad resonance. If the temperature is raised to 50 °C, a singlet at δ = −119 ppm is observed: at this temperature all seven P atoms are equivalent on the NMR time scale. However, below −35 °C the ^{31}P NMR spectrum consists of three separate resonances at δ = −57, −103, and −162 ppm in a 1:3:3 intensity ratio, corresponding to the single phosphorus atom at the apex, the three two-coordinate bridging phosphorus atoms, and the three basal phosphorus atoms, respectively. This temperature dependence is caused by a degenerate Cope rearrangement which has also been observed in the solid state ^{31}P NMR spectra of amorphous $[Li(glyme)]_3P_7$.[3]

It has also been noted that in solution the $[P_7]^{3-}$ cage can act as a Brønsted base capable of deprotonating weakly acidic reagents yielding the di- and monoanionic species $[HP_7]^{2-}$ and $[H_2P_7]^-$.[4] The $[HP_7]^{2-}$ cluster anion has been found to crystallize from solutions of K_3P_7 in ethylenediamine in the presence of a series of cation sequestering agents, indicating that in ethylenediamine a certain amount of the protonated cluster must be present in solution, via deprotonation of the solvent, sequestering agents or adventitious moisture.[4a] This can be corroborated by ^{31}P NMR experiments which show the presence of the $[HP_7]^{2-}$ cluster as two broad resonances at −22.5 and −115.2 ppm in the room temperature ^{31}P NMR spectrum of K_3P_7/2,2,2-crypt mixtures in ethylenediamine.

The earliest reactivity studies of group 15 Zintl anions found that $[E_7]^{3-}$ (E = P, As) could be functionalized yielding neutral trisubstituted adducts such as R_3E_7 (e.g., R = H, ^{n}Bu, $SnMe_3$), a result of the strongly nucleophilic character of the $[E_7]^{3-}$ cages.[5−14] Alkyl exchange reactions or reactions with tetraalkylammonium salts or alkyl tosylates (R_4N^+ and ROTs, respectively) were also found to give disubstituted monoanionic species, $[R_2E_7]^-$ (E = P, As; R = Me, Et, ^{n}Bu, Bz, ^{i}Pr, ^{i}Bu).[15−18]

More recent studies have found that selected transition metal organometallic reagents can also react with $[E_7]^{3-}$ (E = P, As, Sb) cluster anions. In many of the reactions studied, the seven atom cluster cores remain largely intact, yielding products such as $[E_7M(CO)_3]^{3-}$ (E = P, As, Sb; M = Cr, Mo, W),[19,20] $[HP_7M(CO)_3]^{2-}$ (M = Cr, W),[21] $[RP_7W(CO)_3]^{2-}$ (R = Me,

Received: December 16, 2010
Published: March 22, 2011

Et, ^{n}Bu, CH_2Ph),[16] $[R_3EP_7W(CO)_3]^{2-}$ (e.g., $R_3E = Me_3Si$, Et_3Ge, $^n Bu_3Sn$, Ph_3Pb),[22,23] $P_7[FeCp(CO)_2]_3$,[24] $[P_7Ni(CO)]^{3-}$,[25] $[HP_7Ni(CO)]^{2-}$,[25] $[E_7PtH(PPh_3)]^{2-}$ (E = P, As),[25,26] and $[Pd_2As_{14}]^{4-}$.[27] Additional reactions where the anions undergo extensive bond-dissociation and reassembly of the cluster geometries are also possible resulting in intermetallic species such as $[ME_8]^{n-}$ (M = Nb, Cr, Mo; E = As, Sb; n = 2, 3),[28−30] $[Sb_7Ni_3(CO)_3]^{3-}$,[31] $[Ni_5Sb_{17}]^{4-}$,[32] $[Pd_7As_{16}]^{4-}$,[27] and $[As@Ni_{12}@As_{20}]^{3-}$.[33]

The aforementioned studies prompted us to explore the reactivity of $[E_7]^{3-}$ cages toward homoleptic post-transition metal organometallics. Recent studies by our research group have focused on the reactivity of the cluster anions toward Cu_5Mes_5 (Mes =2,4,6-$Me_3C_6H_2$), $M(C_6H_5)_2$ (M = Zn, Cd, Hg) and $In(C_6H_5)_3$ yielding a series of functionalized clusters $[Cu_2E_{14}]^{4-}$, $[ZnE_{14}]^{4-}$, $[CdP_{14}]^{4-}$, and $[E_7InPh_2]^{2-}$ (E = P, As).[34] These findings led us to study the reactivity of such clusters toward the organometallic species $[M(nbe)_3][SbF_6]$ (M = Ag, Au; nbe = norbornene). The results of this research are detailed herein. It yielded two novel cluster anions with unprecedented geometries based on two $[HP_7]^{2-}$ units which are bridged by M^+-M^+ dimers exhibiting metallophilic interactions. These reactions were later optimized by addition of a source capable of protonating the $[P_7]^{3-}$ cages (ammonium tetraphenyborate) and by the replacement of $[M(nbe)_3][SbF_6]$ with commercially available chloride salts of silver(I) and gold(I).

2. EXPERIMENTAL SECTION

All reactions and product manipulations were carried out under an inert atmosphere using standard Schlenk-line or glovebox techniques (MBraun UNIlab glovebox maintained at <0.1 ppm H_2O and <0.1 ppm O_2). Because of the light sensitive nature of many of the reactants and products, where possible, all the containers were covered with aluminum foil to protect them from light. The intermetallic precursor, K_3P_7, was synthesized according to a previously reported synthetic procedure from a mixture of the elements (K: 99.95%, Aldrich; P: 99.99%, Aldrich) heated at 900 °C for 72 h in sealed niobium containers.[35] To avoid the oxidation of the niobium vessels at such temperatures they were jacketed in flame-sealed silica ampules under vacuum prior to heating.

Prior to use, toluene (99.9% Rathburn), hexane (99.9% Rathburn), diethylether (99.9%, Rathburn), dimethylformamide (DMF, 99.9%, Rathburn), tetrahydrofuran (THF, 99.9%, Rathburn), and dichloromethane (HPLC grade, Fisher) were dried using an MBraun MB SPS-800 solvent purification system. Ethylenediamine (99.9% Aldrich) was purified by distillation over sodium metal. d_7-DMF (Cambridge Isotope Laboratories, Inc.) was dried over CaH_2 and vacuum distilled. $CDCl_3$ (99.8% Sigma-Aldrich) was dried over 3 Å molecular sieves (Arcos). All solvents were stored in gastight ampules, under argon. In addition, toluene and diethylether were stored over activated 3 Å molecular sieves (Arcos). 2,2,2-Crypt (4,7,13,16,21,24-hexaoxa-1,10-diazabicyclo[8.8.8] hexacosane; ≥99% Merck) was used as delivered after being carefully dried under vacuum. $Ag[SbF_6]$ (98% Strem), $AuCl(SMe_2)$ (Sigma-Aldrich), AgCl (99.9%, Strem), AuCl (97%, Strem) and bicyclo-[2.2.1]hept-2-ene (norbornene) (99% Sigma-Aldrich) were used as delivered. $[M(nbe)_3][SbF_6]$ (M = Ag, Au) were synthesized using modified literature reported methods (see Supporting Information for full details).[36,37]

Synthesis of $[K(2,2,2\text{-crypt})]_2[Ag_2(HP_7)_2]$ (1). A mixture of K_3P_7 (60 mg, 0.18 mmol), $[Ag(nbe)_3][SbF_6]$ (112 mg, 0.18 mmol), and 2,2,2-crypt (203 mg, 0.54 mmol) were dissolved in 5 mL of ethylenediamine, and the resulting dark orange solution was left to stir for approximately 2 h in a small Schlenk tube. The solution was filtered through a cannula into a dry ampule, and the ruby red filtrate layered with approximately 20 mL of toluene. This mixture was left to crystallize for a week, and approximately 15 mg (∼12% yield) of thin yellow needle-like crystals formed, as well as a reddish precipitate. The crystals were characterized by single crystal X-ray diffraction as $[K(2,2,2\text{-crypt})]_2[Ag_2(HP_7)_2]$. ESI− MS. (DMF): m/z 652.0, $[Ag_2(HP_7)_2]^-$; 691.1, $[KAg_2(HP_7)_2]^-$; 1065.9, $\{[K(2,2,2\text{-crypt})][Ag_2(HP_7)_2]\}^-$; 2547.0, $\{[K(2,2,2\text{-crypt})]_3[Ag_2(HP_7)_2]_2\}^-$. ESI+ MS (DMF): m/z 1895.3, $\{[K(2,2,2\text{-crypt})]_3[Ag_2(HP_7)_2]\}^+$.

Alternate Synthesis of 1. A second, improved, method was devised to synthesize **1** in greater yields. A mixture of K_3P_7 (97 mg, 0.29 mmol), AgCl (53 mg, 0.37 mmol), 2,2,2-crypt (225 mg, 0.60 mmol), and $[NH_4][BPh_4]$ (99 mg, 0.29 mmol) were dissolved in approximately 2 mL of ethylenediamine to form a brown solution which was stirred under argon for approximately 3 h. The solvent was removed under a dynamic vacuum to leave a brown solid which was washed twice with approximately 10 mL of THF and sonicated in an attempt to dissolve the chloride and tetraphenylborate salt byproducts. The THF fractions were filtered off and disposed of, and the remaining solid residue was dried under vacuum yielding 89.7 mg (42% yield) of **1**. Anal. Calcd. for $Ag_2P_{14}K_2C_{36}H_{74}N_4O_{12}$: C 29.16%, H 5.03%, N 3.78%. Found: C 28.70%, H 4.65%, N 3.92%. ESI− MS (DMF): m/z 652.5 $[Ag_2(HP_7)_2]^-$, 690.5 $[KAg_2(HP_7)_2]^-$, 1066.7 $\{[K(2,2,2\text{-crypt})][Ag_2(HP_7)_2]\}^-$. ESI+ MS (DMF): m/z 1897.0 $\{[K(2,2,2\text{-crypt})]_3[Ag_2(HP_7)_2]\}^+$. ^{1}H NMR data (500 MHz, d_7-DMF): δ (ppm) 3.59 (24H, s, 2,2,2-crypt), 3.56 (24H, t, 2,2,2-crypt, $^3J_{H-H}$ = 4.7 Hz), 2.54 (24H, t, 2,2,2-crypt, $^3J_{H-H}$ = 4.7 Hz). ^{31}P NMR data (125.0 MHz, d_7-DMF): δ (ppm): 60.9 (m, $[P_{16}]^{2-}$), 39.1 (m, $[P_{16}]^{2-}$), 17.9 (1P, broad m, P2 or P3), 7.7 (1P, m, P2 or P3, $^1J_{P-P}$ = 402 Hz, $^1J_{P-P}$ = 380 Hz − this resonance partially overlaps with a resonance corresponding to $[P_{16}]^{2-}$), −33.7 (1P, broad m, P4 − this resonance partially overlaps with a resonance corresponding to $[P_{16}]^{2-}$), −40.5 (1P, m, P1, $^1J_{P-P}$ = 380 Hz), −86.6 (1P, m, P7, $^1J_{P-P}$ =250 Hz), −132.8 (m, $[P_{16}]^{2-}$), −171.7 (m, $[P_{16}]^{2-}$), −197.3 (1P, broad m, P5 or P6), −212.7 (1P, m, P5 or P6, $^1J_{P-P}$ = 250 Hz, $^1J_{P-P}$ = 202 Hz), −240.6 (quartet, PH_3, $^1J_{P-H}$ = 189 Hz).

Synthesis of $[K(2,2,2\text{-crypt})]_2[Au_2(HP_7)_2]$ (2). A mixture of K_3P_7 (45.7 mg, 0.137 mmol), $[Au(nbe)_3][SbF_6]$ (105 mg, 0.147 mmol), and 2,2,2-crypt (109 mg, 0.290 mmol) were dissolved in 5 mL of ethylenediamine, and the resulting dark brown solution left to stir for approximately 2 h in a small Schlenk tube. The solution was filtered through a filter cannula into an ampule, and the bright yellow filtrate was layered with approximately 20 mL of toluene. The mixture was left to crystallize for a week yielding approximately 10 mg (∼15% yield) of pale yellow plate-like crystals. These crystals were characterized by single crystal X-ray diffraction as $[K(2,2,2\text{-crypt})]_2[Au_2(HP_7)_2]$. ESI− MS (DMF): m/z 830.7, $[Au_2(HP_7)_2]^-$; 868.8, $[KAu_2(HP_7)_2]^-$; 1245.0, $\{[K(2,2,2\text{-crypt})][Au_2(HP_7)_2]\}^-$. ESI+ MS (DMF): m/z 2074.7, $\{[K(2,2,2\text{-crypt})]_3[Au_2(HP_7)_2]\}^+$.

Alternate Synthesis of 2. A mixture of K_3P_7 (96 mg, 0.29 mmol), AuCl (69 mg, 0.30 mmol), 2,2,2-crypt (220 mg, 0.59 mmol), and $[NH_4][BPh_4]$ (96.7 mg, 0.29 mmol) were dissolved in approximately 2 mL of ethylenediamine to form a brown solution which was stirred under argon for approximately 3 h. The solvent was removed under a dynamic vacuum to leave a brown solid which was washed twice with approximately 10 mL of THF and sonicated in an attempt to dissolve the chloride and tetraphenylborate salt byproduct. The THF fractions were filtered off and disposed of, and the remaining solid residue was dried under vacuum yielding 146 mg (61% yield) of **2**. Anal. Calcd. for $C_{36}H_{74}Au_2K_2N_4O_{12}P_{14}$: C 26.02; H 4.49; N 3.37. Found: C 25.83; H 4.37; N 3.22. ESI− MS (DMF): m/z 830.4 $[Au_2(HP_7)_2]^-$, 868.3 $[KAu_2(HP_7)_2]^-$, 1244.4 $\{[K(2,2,2\text{-crypt})][Au_2(HP_7)_2]\}^-$. ESI+ MS

(DMF): m/z 2074.5 $\{[K(2,2,2\text{-crypt})]_3[Au_2(HP_7)_2]\}^+$. ^{1}H NMR (500.0 MHz, d_7-DMF): δ (ppm) 3.59 (24H, s, 2,2,2-crypt), 3.57 (24H, t, 2,2,2-crypt, $^3J_{H-H}$ = 4.7 Hz), 2.55 (24H, t, 2,2,2-crypt, $^3J_{H-H}$ = 4.7 Hz). ^{31}P NMR (125.0 MHz, d_7-DMF): δ (ppm) 83.8 (1P, m, P2 or P3, $^1J_{P-P}$ = 315 Hz, $^1J_{P-P}$ = 335 Hz), 60.6 (m, $[P_{16}]^{2-}$), 50.3 (1P, m, P2 or P3, $^1J_{P-P}$ = 347 Hz, $^1J_{P-P}$ = 315 Hz), 38.8 (m, $[P_{16}]^{2-}$), 6.8 (m, $[P_{16}]^{2-}$), −22.4 (1P, broad m, P4), −34.0 (m, $[P_{16}]^{2-}$), −92.1 (1P, m, P1, $^1J_{P-P}$ = 315 Hz, $^1J_{P-P}$ = 295 Hz), −133.0 (m, $[P_{16}]^{2-}$), −154.0 (1P, broad m, P7), −171.9 (m, $[P_{16}]^{2-}$), −212.8 (1P, m, P5 or P6, $^1J_{P-P}$ = 260 Hz, $^1J_{P-P}$ = 203 Hz, $^1J_{P-P}$ = 335 Hz), −228.5 (1P, broad m, P5 or P6), −240.8 (quartet, PH_3, $^1J_{P-H}$ = 189 Hz).

Single Crystal X-ray Structure Determination. Single crystal X-ray diffraction data were collected on an Enraf-Nonius Kappa CCD diffractometer. Crystals were selected under Paratone-N oil, mounted on micromount loops, and quench-cooled using an open flow N_2 cooling device.[38] Data were collected at 150 K using graphite monochromated Mo Kα radiation and processed using the DENZO-SMN package, including unit cell parameter refinement and interframe scaling (which was carried out using SCALEPACK within DENZO-SMN).[39] The structures were solved by direct methods using SHELXS,[40] and refined on F using CRYSTALS.[41] Most hydrogen atoms were visible in the difference map, and their positions and isotropic displacement parameters were refined using restraints prior to inclusion into the model with riding constraints.[42] Data for a second polymorph of **1** (**1b**) were collected on beamline I19 at the Diamond Light Source, Didcot; however, the crystals were of poor quality and the results are only included in the final .cif file for completeness. The final refinements were weighted using a Chebychev polynomial weighting scheme.[43]

Computational Methods. All calculations described in this paper were performed using the Amsterdam Density Functional package (ADF2007.01).[44] A triple-ζ Slater-type basis set, extended with a single polarization function, was used to describe all atoms. The local density approximation was employed for the optimizations,[45] along with the local exchange-correlation potential of Vosko, Wilk, and Nusair[46] and gradient corrections to exchange and correlation proposed by Becke and Perdew (BP86).[47] Relativistic effects were incorporated using the Zeroth Order Relativistic Approximation (ZORA).[48] The presence of cations in the crystal lattice of **1** was modeled by surrounding the anion with a continuum dielectric using COSMO.[49] The chosen dielectric constant ε = 16.9 corresponds to that of ammonia, although structural parameters are not strongly dependent on this choice. All structures were optimized using the gradient algorithm of Versluis and Ziegler.[50]

Electrospray Mass-Spectrometry. Positive and negative ion mode electrospray mass spectra were recorded from DMF solutions (10−20 μM) on a Masslynx LCT Time of Flight mass spectrometer with a Z-spray source (150 °C source temperature, 200 °C desolvation temperature, 2.4 kV capillary voltage and 25 V cone voltage). The samples were introduced directly with a 1 mL SGE syringe and a syringe pump at 0.6 mL/h.

NMR. ^{1}H and ^{31}P NMR spectra were acquired at 500.0 and 125.0 MHz, respectively, on a Varian Unity-plus 500 NMR spectrometer. ^{1}H spectra were referenced to the most downfield residual protic solvent resonance (DMF δ 8.03 ppm). ^{31}P spectra were externally referenced to H_3PO_4 (δ 0 ppm).

Elemental Analyses. CHN elemental analyses were performed on 5 mg samples submitted under vacuum in flame-sealed Pyrex ampules.

3. RESULTS AND DISCUSSION

Reactions of ethylenediamine solutions of K_3P_7 with $[M(nbe)_3][SbF_6]$ (M = Ag, Au; nbe = norbornene) in a 1:1 ratio in the presence of 2,2,2-crypt yielded the compounds $[K(2,2,2\text{-crypt})]_2[M_2(HP_7)_2]$ (M = Ag (**1**), Au (**2**)). These species, and the $[M(nbe)_3][SbF_6]$ precursors, are light sensitive and must be manipulated in the dark. Left standing in the light, solutions of **1** and **2** decompose to the known cluster anions $[HP_7]^{2-}$ and $[P_{16}]^{2-}$, as well as to colloidal solutions and precipitates of the coinage metals. **1** and **2** were obtained in low crystalline yields (approximately 15%) from ethylenediamine/toluene solvent mixtures and characterized by single crystal X-ray diffraction. The crystal structures of **1** and **2** contain a single $[K(2,2,2\text{-crypt})]^+$ cation and half of a $[M_2(HP_7)_2]^{2-}$ cluster dianion in their respective asymmetric units (a crystallographic center of inversion is located at the central point of the M^+-M^+ bond). Details of the crystallographic data are given in Table 1.[51]

Table 1. Selected X-ray Data Collection and Refinement Parameters for $[K(2,2,2\text{-crypt})]_2[Ag_2(HP_7)_2]$ (1) and $[K(2,2,2\text{-crypt})]_2[Au_2(HP_7)_2]$ (2)

	1	2
chemical formula	$C_{18}H_{37}AgKN_2O_6P_7$	$C_{18}H_{37}AuKN_2O_6P_7$
Fw	741.28	830.38
crystal system	monoclinic	monoclinic
space group, Z	$P2(1)/c$, 4	$P2/n$, 4
a (Å)	10.7536(1)	14.4130(2)
b (Å)	27.0054(2)	10.8462(2)
c (Å)	10.6651(1)	19.9351(4)
α (deg)	90.00	90.00
β (deg)	92.336(1)	102.8771(1)
γ (deg)	90.00	90.00
V (Å^3)	3094.63(5)	3038.00(9)
ρ_{calc} (g cm^{-3})	1.591	1.815
radiation, λ (Å), temp (K)	Mo K$_\alpha$, 0.71073, 150	
μ (mm^{-1})	1.182	5.383
no. refined parameters	316	321
reflections collected	57032	66526
unique reflections (R_{int})	7032 (0.029)	6906 (0.113)
R_1/wR_2,[a] $I \geq 2\sigma_I$ (%)	3.13/6.00	4.88/12.89
R_1/wR_2,[a] all data (%)	5.82/7.83	8.19/14.17

[a] $R_1 = [\Sigma||F_o| - |F_c||]/\Sigma|F_o|$; $wR_2 = \{[\Sigma w(F_o^2 - F_c^2)^2]/[\Sigma w(F_o^2)^2]\}^{1/2}$.

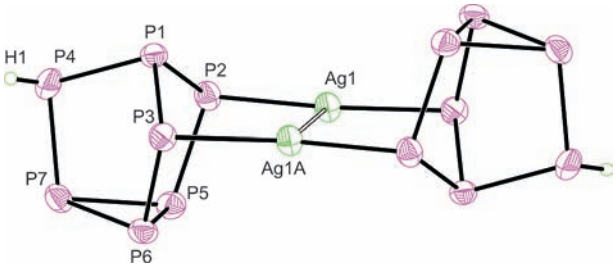

Figure 1. Thermal ellipsoid plot of the $[Ag_2(HP_7)_2]^{2-}$ cluster anion present in sample **1**. Anisotropic displacement ellipsoids pictured at 50% probability level. A crystallographic center of inversion is located at the central point between Ag1 and Ag1A. Ag1−Ag1A bond distance: 2.947(1) Å.

Solid-State Structures. The cluster anions present in **1** and **2** are largely isostructural (see Figures 1 and 2). Each cluster exhibits a M_2^{2+} dimer which is bridged by two $[HP_7]^{2-}$ cages, $[M_2(\mu^2\text{-}HP_7)_2]^{2-}$, conferring the overall cluster anion pseudo C_{2h} point symmetry (if the positions of the hydrogen atoms are

dx.doi.org/10.1021/ic102516g |Inorg. Chem. 2011, 50, 4021–4028

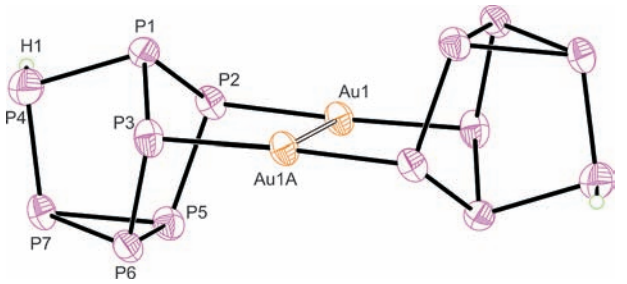

Figure 2. Thermal ellipsoid plot of the $[Au_2(HP_7)_2]^{2-}$ cluster anion present in sample **2**. Anisotropic displacement ellipsoids pictured at 50% probability level. A crystallographic center of inversion is located at the central point between Au1 and Au1A. Au1−Au1A bond distance: 3.047(1) Å.

Table 2. Selected Bond Distances (Å) and Angles (deg) for $[K(2,2,2\text{-crypt})]_2[Ag_2(HP_7)_2]$ (1) and $[K(2,2,2\text{-crypt})]_2[Au_2(HP_7)_2]$ (2)

	1	2
P1−P2	2.177(1)	2.184(3)
P1−P3	2.176(1)	2.175(3)
P1−P4	2.181(1)	2.185(3)
P2−P5	2.174(1)	2.177(3)
P3−P6	2.164(1)	2.175(3)
P4−P7	2.195(1)	2.183(3)
P5−P6	2.236(1)	2.224(3)
P5−P7	2.237(1)	2.220(3)
P6−P7	2.230(1)	2.217(3)
M1−M1A	2.947(1)	3.047(1)
M1−P2	2.411(1)	2.357(2)
M1−P3	2.415(1)	2.349(2)
P4−H1	1.27(8)	1.14(9)
P1−P4−H1	107(4)	97(4)
P7−P4−H1	105(3)	122(4)
P2−M1−P3	167.00(3)	169.42(7)
P2−M1−M1A	95.56(2)	94.31(5)
P3−M1−M1A	97.41(2)	96.24(5)

ignored). Each M atom has a "T-shaped" coordination environment, exhibiting a close contact to the other (symmetry related) M atom and two bonds to phosphorus atoms from adjacent cages. The two bridging M atoms and the phosphorus atoms which comprise their immediate coordination sphere are coplanar and give rise to an "H-shaped" motif (mean deviations from planes are 0.007 and 0.006 Å for the M1/M1A/P2/P3/P2A/P3A atoms in **1** and **2**, respectively). A comparison of bond distances and angles for each of the cluster anions is provided in Table 2. The structures of the $[M_2(HP_7)_2]^{2-}$ anions are closely related to the $[P_{16}]^{2-}$ cage which has been previously reported in the literature.[52] There are, however, significant differences between these two species as highlighted in Figure 3. The most significant is that the structure of $[P_{16}]^{2-}$ is "bent" along the two phosphorus atoms which bridge the heptaphosphide moieties (atoms P8 and P9 according to the numbering scheme employed in Figure 3). An additional difference is that in $[P_{16}]^{2-}$, the apical P1 atoms of the P_7 cages point in the same direction (an "up−up" isomer), whereas in the two $[M_2(HP_7)_2]^{2-}$ anions they point in

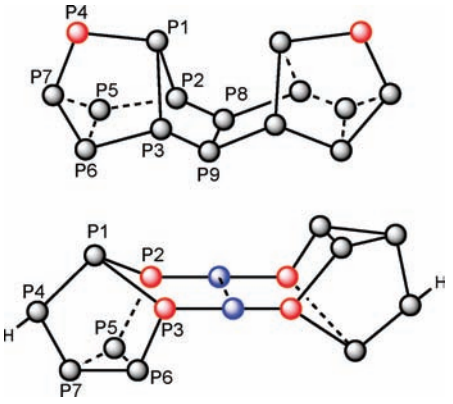

Figure 3. Comparison of the structures of $[P_{16}]^{2-}$ (top) and $[M_2(HP_7)_2]^{2-}$ (bottom). Atoms colored in red carry a formal negative charge, whereas blue atoms represent positively charged Ag^+ or Au^+ ions.

opposite directions ("up−down" isomers). There is no clear motive why we have only been able to observe the "up−down" isomer crystallographically, and we can only assume that subtle crystal packing effects must play a significant role. In steric terms, the "up−up" isomer would seem just as viable, and density functional theory (DFT) calculations indicate that there is no significant difference in the total bonding energies for the optimized geometries of both isomers (ΔE values between the "up−up" and "up−down" isomers are 0.4 and 2.4 kJ mol^{-1} for $[Ag_2(HP_7)_2]^{2-}$ and $[Au_2(HP_7)_2]^{2-}$, respectively and therefore within the range of computational error). Full details of DFT computations are provided in the Supporting Information. By contrast the hypothetical "up−down" isomer of $[P_{16}]^{2-}$ would exhibit significant steric repulsion between adjacent heptaphosphido moieties.

The protic positions of the $[M_2(HP_7)_2]^{2-}$ cages present in **1** and **2** were determined by studying the residual electron density in the asymmetric unit of the crystal structures after all atomic positions had been determined and refined anisotropically and initial hydrogen positions of the $[K(2,2,2\text{-crypt})]^+$ cations had been determined. Crystallographically determining whether the clusters are protonated and if so, where the protons are located can be challenging and is increasingly difficult in the presence of heavy atoms.[42] In both **1** and **2** some of the largest residual Q-peaks were observed at chemically viable positions in close proximity to the P4 atoms (see Figures 1 and 2). The atomic coordinates and isotropic temperature factors of the hydrogen atoms in the cluster were freely refined, and the overall fit of the model to the data was found to improve on incorporation of the protons. The final positions of these atoms were found to be consistent with a trigonal pyramidal coordination environment at the P4 atoms. Additional studies truncating the data to 0.22 $Å^{-2}$ $(\sin\theta/\lambda)^2$ also helped corroborate the positioning of these protons (see Supporting Information for full details).

The internuclear Ag−Ag distance in **1**, 2.947(1) Å, is slightly shorter than the average of the 101 structures in the Cambridge Structural Database (CSD) which contain a Ag−Ag contact and where each metal atom is 3-coordinate (3.018(18) Å).[53] For a similar search, restricted to species in which the silver atoms are formally in the +1 oxidation state, unsurprisingly the average distance is longer 3.087(26) Å (based on 43 hits). A closely related species, $[Ag_2(\mu^2\text{-dcpm})_2](PF_6)_2$ (dcpm = bis(dicyclohexylphosphino)methane) also contains silver in a

dx.doi.org/10.1021/ic102516g |*Inorg. Chem.* 2011, 50, 4021–4028

"T-shaped" coordination environment with ligated phosphorus atoms and has a Ag(I)−Ag(I) internuclear distance of 2.938(1) Å.[54] The relatively short Ag1−Ag1A distance observed in **1** can be considered indicative of a closed-shell "argentophilic" interaction between two d^{10} silver metal centers.[55]

Similarly, a search of the CSD highlighted 242 species with structures containing three-coordinate gold atoms and an Au−Au interaction.[53] The average distance for these interactions was 3.037(9) Å, which is in good agreement with the Au−Au distance of 3.047(1) Å found in $[Au_2(HP_7)_2]^{2-}$. As a reference, the structure of $[Au_2(\mu^2\text{-dmpm})_2]Br_2\cdot 2H_2O$ (dmpm = 1,2-bis-(dimethylphosphino)methane)) contains the same arrangement of phosphorus atoms around a Au(I)−Au(I) dimer and exhibits an interatomic Au−Au contact of 3.023(1) Å.[56] This distance is comparable to that present in the crystal structure of **2**, and consistent with an "aurophilic" interaction.[56,57] Such interactions were first reported by Schmidbauer and co-workers and are believed to be dispersion forces of the same order of magnitude as hydrogen bonding interactions (29 to 46 kJ/mol).[58] Metal−metal distances in such complexes are strongly influenced by the nature and bite angle of bridging ligands, and as a result a meaningful discussion of internuclear distances, and the relative strength of such interactions, can prove challenging. Interestingly, **1** and **2** represent one of the few series of compounds where the chemical environment about the metallophilic interaction remains constant and therefore allows for a direct comparison of Ag−Ag and Au−Au distances. Our data suggest that, all other factors being equal, the Au(I)−Au(I) distance is only 0.1 Å longer than the Ag(I)−Ag(I) bond. That being said, very little information should be extrapolated with respect to the relative strength of these interactions as other factors, such as crystal packing effects, may also influence the observed interatomic metal−metal distances. Theoretical considerations suggest that relativistic effects and s-d hybridization should increase the relative strength of the gold(I)−gold(I) interaction relative to related interactions between silver(I) ions. Therefore, it seems counterintuitive that the M−M interaction should be shorter in **1** than in **2**.[58] Interestingly, a similar effect has been previously observed for a series of $[M(NH_3)_2]^+$ salts (M = Ag, Au).[59] In these species, the M−M distances of the gold adduct were also found to be longer than in the silver analogue and the M−N distances shorter. This is also observed in the $[Au_2(HP_7)_2]^{2-}$ cluster anions where the M−P distances are ever so slightly shorter in **2** relative to **1** (2.353 (av) Å vs 2.413 (av) Å, respectively).

Theoretical calculations were found to mirror the observed structural differences between $[Ag_2(HP_7)_2]^{2-}$ and $[Au_2(HP_7)_2]^{2-}$. The optimized cluster geometries were calculated using DFT methods, and the computed bond distances and angles show a good correlation with crystallographically determined values (see Supporting Information for full details). The calculated Ag−Ag and Au−Au interatomic distances are 3.057 and 3.238 Å, respectively. Similarly, M−P distances in the computed geometries were found to be 2.439 and 2.386 Å, for the Ag and Au species, respectively. These values are consistent with the longer M−M interactions and shorter M−P bonds observed in $[Au_2(HP_7)_2]^{2-}$ relative to its silver homologue. These computed interatomic distances are slightly longer than the crystallographically determined values, in all likelihood as a result of the simplistic method used to model the crystal environment for the cluster anions, which was simulated using a continuum dielectric. Comparison with single point calculations using the atomic coordinates as determined by single crystal X-ray diffraction, suggest that the elongation of the bonds in the optimized structures introduces no significant changes to the shapes or relative energies of the frontier orbitals.

Scheme 1. Proposed Equilibrium between a Brønsted Acid and $[P_7]^{3-}$ to Give $[HP_7]^{2-}$ and the Corresponding Conjugate Base[a]

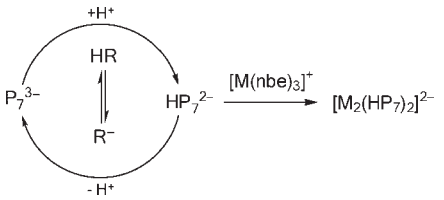

[a] Reactions between the protonated cluster anions and homoleptic M^+ (M = Ag, Au) organometallics yield **1** and **2**.

Solution Reactivity Studies. The cluster anions present in **1** and **2** can be interpreted from an electron counting perspective as being formally composed of an M_2^{2+} core (a recurring motif in the chemistry of the heavier group 11 elements) and two $[HP_7]^{2-}$ cages, thus conferring the overall clusters the 2− charges determined by single crystal X-ray diffraction. Related clusters containing a Cu_2^{2+} core, $[Cu_2(E_7)_2]^{4-}$ (E = P, As) were recently reported by our research group, and found to carry a 4− charge.[34] In these species there was no evidence of cluster protonation, and the geometry observed was markedly different from that exhibited by the $[M_2(HP_7)_2]^{2-}$ anions present in **1** and **2**. For the $[M_2(HP_7)_2]^{2-}$ anions to form, it is necessary that the heptaphosphide $[P_7]^{3-}$ cages, or the as of yet unobserved $[M_2(P_7)_2]^{4-}$ anions, abstract a proton(s) from the solvent (or other possible protic species such as adventitious moisture). A schematic representation of this process is pictured in Scheme 1. Previous reports suggest that the role of 2,2,2-crypt in such processes may not be entirely innocent and that abstracted hydrogen in closely related cluster anions may originate from the sequestering agent.[21] This is supported by studies which have reported the isolation of crystalline samples of $[HP_7]^{2-}$ from ethylenediamine solutions of K_3P_7 and 2,2,2-crypt.[4a]

To date we have observed no indication of any reactivity between the $[P_7]^{3-}$ precursor and the $[M(nbe)_3][SbF_6]$ reagents, that is, no formation of the nonprotonated species $[M_2(P_7)_2]^{4-}$, despite the fact that the copper analogue has been previously reported.[34] This would make it seem that formation of the $[HP_7]^{2-}$ intermediate is necessary prior to the synthesis of $[M_2(HP_7)_2]^{2-}$. Low concentrations of $[HP_7]^{2-}$ in solution may account for the low yields obtained for the syntheses of **1** and **2** in the absence of any protic reagents. We have tested this hypothesis by attempting to increase the relative concentration of $[HP_7]^{2-}$ in solution prior to the addition of the metal precursor.

Dissolution of K_3P_7 and 2,2,2-crypt in ethylenediamine was followed by the addition of a stoichiometric amount of ammonium tetraphenylborate which yielded the $[HP_7]^{2-}$ cluster anion as evidenced by $^{31}P\{^1H\}$ and ^1H NMR spectroscopy. Addition of 1 equivalent of $[Ag(nbe)_3][SbF_6]$ or $[Au(nbe)_3][SbF_6]$ to such a mixture was found to yield the $[Ag_2(HP_7)_2]^{2-}$ and $[Au_2(HP_7)_2]^{2-}$ cluster anions, respectively. These species could be isolated in much higher yields than in the absence of the ammonium salt (approximately 50%). This observation indicates that formation of the protonated cluster cages $[HP_7]^{2-}$ prior to the addition of the metal salt precursors strongly favors the

dx.doi.org/10.1021/ic102516g |Inorg. Chem. 2011, 50, 4021–4028

Scheme 2. Optimized Synthesis of 1 and 2

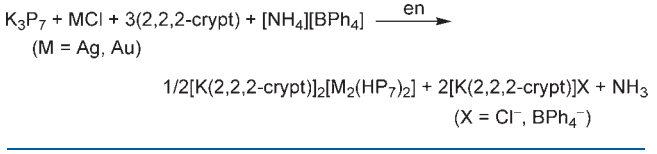

formation of the metal-bridged cluster adducts. It was later observed that **1** and **2** could be obtained using an identical methodology but replacing the norbornadiene adducts of silver(I) and gold(I) by the commercially available chloride salts AgCl and AuCl. This greatly simplifies the procedure for the synthesis of **1** and **2** as the highly reactive homoleptic organometallic reagents $[M(nbe)_3][SbF_6]$ (M = Ag, Au) are no longer required. A balanced stoichiometric reaction for this optimized process is provided in Scheme 2.

Characterization of the $[M_2(HP_7)_2]^{2-}$ (M = Ag, Au) cluster anions in solution by means of NMR spectroscopy proved extremely difficult because of the exceptional sensitivity of the cluster anions toward light, air, and moisture. Numerous attempts at recording the ^1H and ^{31}P NMR spectra of the cluster anions were made; however, these frequently showed evidence of cluster decomposition and formation of $[P_{16}]^{2-}$ and PH_3 as reaction side products. Despite this, however, over the course of multiple NMR experiments we were able to observe consistent and reproducible evidence of the presence of $[Ag_2(HP_7)_2]^{2-}$ and $[Au_2(HP_7)_2]^{2-}$ in solutions of **1** and **2**, respectively. Such solutions show seven multiplet resonances in their ^{31}P NMR spectra which do not correspond to known polyphosphide cluster anions and which are consistent with the cluster geometries as determined by single crystal X-ray diffraction (in addition to resonances arising from other phosphorus-containing impurities). Of these spectra the most well resolved was obtained for sample **2** and showed seven resonances of equal intensity corresponding to the seven inequivalent phosphorus nuclei in $[Au_2(HP_7)_2]^{2-}$. These were observed at 83.8 (P2 or P3), 50.3 (P2 or P3), −22.4 (P4), −92.1 (P1), −154.0 (P7), −212.8 (P5 or P6), −228.5 (P5 or P6) ppm (NMR spectra are provided in the Supporting Information). As with other protonated heptaphosphide cages there is no spectroscopic evidence of inversion of the proton at the P4 position.[21] The ^{31}P NMR spectrum of sample **1** also showed seven similar, albeit less well-resolved, resonances at 17.9 (P2 or P3), 7.7 (P2 or P3), −33.7 (P4), −40.5 (P1), −86.6 (P7), −197.3 (P5 or P6), and −212.7 (P5 or P6) ppm. Several resonances were found to partially overlap with those of the $[P_{16}]^{2-}$ cluster anion which was observed as the principal product. All attempts to observe the proton resonances from the protonated cluster cages proved unsuccessful.

The $[M_2(HP_7)_2]^{2-}$ (M = Ag, Au) clusters were also characterized in solution by positive and negative ion mode ESI− MS. In the negative ion mode spectra, the clusters were observed with reduced charges as a result of the oxidation of the parent cluster anions, presumably arising as a result of the electrical potential difference applied to samples during the ionization process. Both positive and negative ion mode spectra showed evidence of extensive ion pairing between anions and charge-balancing cations such as K^+ and $[K(2,2,2\text{-crypt})]^+$. Negative ion mode spectra of solutions of **1** showed signals at the following m/z values: 652.5, 690.5, and 1066.7, corresponding to $[Ag_2(HP_7)_2]^-$, $\{K[Ag_2(HP_7)_2]\}^-$, and $\{[K(2,2,2\text{-crypt})][Ag_2(HP_7)_2]\}^-$, respectively. Similarly, the positive ion mode revealed a peak at 1897.0 corresponding to the ion-paired species $\{[K(2,2,2\text{-crypt})]_3[Ag_2(HP_7)_2]\}^+$. ESI-MS measurements of sample **2** also revealed peaks corresponding to related cluster anions. The negative ion mode spectra showed mass-envelopes with m/z values of 830.4, 868.3, and 1244.4, corresponding to $[Au_2(HP_7)_2]^-$, $\{K[Au_2(HP_7)_2]\}^-$, and $\{[K(2,2,2\text{-crypt})][Au_2(HP_7)_2]\}^-$. Positive ion mode mass-spectrometry revealed a mass-envelope at 2074.5, arising from the $\{[K(2,2,2\text{-crypt})]_3[Au_2(HP_7)_2]\}^+$ ion pair. These measurements and the aforementioned ^{31}P NMR studies clearly show that the $[M_2(HP_7)_2]^{2-}$ (M = Ag, Au) cluster anions maintain their structural integrity in solution.

4. CONCLUSIONS

In this study we have demonstrated that the hydrogenheptaphosphide dianion, $[HP_7]^{2-}$, is capable of acting as a bridging ligand between two metal centers in a μ^2-η^2 fashion, thus helping to stabilize metallophilic interactions between silver and gold metal centers. This coordination mode, while common for many bidentate ligand systems (such as phosphines), has previously never been observed for any of the heptapnictide cages of group 15. The closely related $[Pd_2As_{14}]^{4-}$ anion can best be described as $[Pd_2(\mu^2\text{-}\eta^2,\eta'^2\text{-}As_7)_2]^{4-}$ with the $[As_7]^{3-}$ anions showing structural evidence of a nortricyclane to norbornadiene-like structural activation.[27] Furthermore these studies hint at the possibility of using salt metathesis reactions between Zintl phases and commercially available metal halide salts as a versatile route to heteroatomic cluster anions of varying compositions. This method has the added advantage that it does not require low valent, low coordinate organometallic reagents of labile or hemilabile ligands, thus greatly simplifying reaction methodologies. Research aimed at expanding these findings is currently underway.

■ ASSOCIATED CONTENT

Supporting Information. X-ray crystallographic files in CIF format. Full experimental and computational details and NMR and ES-MS spectra. This material is available free of charge via the Internet at http://pubs.acs.org.

■ AUTHOR INFORMATION

Corresponding Author
*E-mail: jose.goicoechea@chem.ox.ac.uk.

■ ACKNOWLEDGMENT

We thank the University of Oxford and the EPSRC (DTA studentship C.M.K.) for financial support of this research. We also thank Steve Boyer (London Metropolitan University) for performing all elemental analyses and the Oxford Supercomputing Centre (OSC) for access to instrumentation. Finally, we also thank the Diamond Light Source for the award of beam-time on I19 (MT1858) and Dr. Kirsten E. Christensen and Dr. David R. Allan for their assistance with data collection and refinement for sample **1b**.

■ REFERENCES

(1) Kolis, J. W.; Young, D. M. In *Chemistry, Structure and Bonding of Zintl Phases and Ions*; Kauzlarich, S. M., Ed.; Wiley-VCH: New York, 1996; pp 225−244.

(2) Baudler, M. *Angew. Chem., Int. Ed. Engl.* **1982**, *21*, 492.
(3) Sen, T.; Poupko, R.; Fleischer, U.; Zimmermann, H.; Luz, Z. *J. Am. Chem. Soc.* **2000**, *122*, 889.
(4) (a) Dai, F.-R.; Xu, L. *Inorg. Chim. Acta* **2006**, *359*, 4265. (b) Korber, N.; von Schnering, H. G. *Chem. Commun.* **1995**, 1713. (c) Korber, N.; von Schnering, H. G. *Angew. Chem., Int. Ed. Engl.* **1996**, *35*, 1107. (d) Korber, N.; Daniels, J. *Inorg. Chem.* **1997**, *36*, 4906. (e) Aschenbrenner, J. C.; Korber, N. *Z. Anorg. Allg. Chem.* **2004**, *630*, 31.
(5) Hönle, W.; von Schnering, H. G. *Z. Anorg. Allg. Chem.* **1978**, *440*, 171.
(6) Baudler, M.; Ternberger, H.; Faber, W.; Hahn, J. *Z. Naturforsch.* **1979**, *34B*, 1690.
(7) Baudler, M.; Faber, W.; Hahn, J. *Z. Anorg. Allg. Chem.* **1980**, *469*, 15.
(8) Fritz, G.; Hoppe, K. D.; Hönle, W.; Weber, D.; Mujica, C.; Manriquez, V.; von Schnering, H. G. *J. Organomet. Chem.* **1983**, *249*, 63.
(9) Baudler, M. *Angew. Chem., Int. Ed.* **1987**, *26*, 419.
(10) von Schnering, H. G.; Hönle, W. *Chem. Rev.* **1988**, *88*, 243.
(11) Fritz, G.; Schneider, H.-W. *Z. Anorg. Allg. Chem.* **1990**, *584*, 12.
(12) Fritz, G.; Layher, E.; Goesmann, H.; Hanke, D.; Persau, C. *Z. Anorg. Allg. Chem.* **1991**, *594*, 36.
(13) Kovács, I.; Baum, G.; Fritz, G.; Fenske, D.; Wiberg, N.; Schuster, H.; Karaghiosoff, K. *Z. Anorg. Allg. Chem.* **1993**, *619*, 453.
(14) Baudler, M.; Glinka, K. *Chem. Rev.* **1993**, *93*, 1623.
(15) Fritz, G.; Harer, J.; Matern, E. *Z. Anorg. Allg. Chem.* **1983**, *504*, 38.
(16) Charles, S.; Fettinger, J. C.; Eichhorn, B. W. *J. Am. Chem. Soc.* **1995**, *117*, 5303.
(17) Mattamana, S. P.; Promprai, K.; Fettinger, J. C.; Eichhorn, B. W. *Inorg. Chem.* **1998**, *37*, 6222.
(18) Milyukov, V. A.; Kataev, A. V.; Hey-Hawkins, E.; Sinyashin, O. G. *Russ. Chem. Bull.* **2007**, *56*, 298.
(19) Eichhorn, B. W.; Haushalter, R. C.; Huffman, J. C. *Angew. Chem., Int. Ed.* **1989**, *28*, 1032.
(20) Charles, S.; Eichhorn, B. W.; Rheingold, A. L.; Bott, S. G. *J. Am. Chem. Soc.* **1994**, *116*, 8077.
(21) Charles, S.; Danis, J. A.; Mattamana, S. P.; Fettinger, J. C.; Eichhorn, B. W. *Z. Anorg. Allg. Chem.* **1998**, *624*, 823.
(22) Charles, S.; Danis, J. A.; Fettinger, J. C.; Eichhorn, B. W. *Inorg. Chem.* **1997**, *36*, 3772.
(23) Kesanli, B.; Mattamana, S. P.; Danis, J.; Eichhorn, B. *Inorg. Chim. Acta* **2005**, *358*, 3145.
(24) Ahlrichs, R.; Fenske, D.; Fromm, K.; Krautscheid, H.; Krautscheid, U.; Treutler, O. *Chem.—Eur. J.* **1996**, *2*, 238.
(25) Charles, S.; Fettinger, J. C.; Bott, S. G.; Eichhorn, B. W. *J. Am. Chem. Soc.* **1996**, *118*, 4713.
(26) Kesanli, B.; Charles, S.; Lam, Y. F.; Bott, S. G.; Fettinger, J.; Eichhorn, B. *J. Am. Chem. Soc.* **2000**, *122*, 11101.
(27) Moses, M. J.; Fettinger, J.; Eichhorn, B. *J. Am. Chem. Soc.* **2002**, *124*, 5944.
(28) Kesanli, B.; Fettinger, J.; Scott, B.; Eichhorn, B. *Inorg. Chem.* **2004**, *43*, 3840.
(29) Eichhorn, B. W.; Mattamana, S. P.; Gardner, D. R.; Fettinger, J. C. *J. Am. Chem. Soc.* **1998**, *120*, 9708.
(30) Kesanli, B.; Fettinger, J.; Eichhorn, B. *J. Am. Chem. Soc.* **2003**, *125*, 7367.
(31) Charles, S.; Eichhorn, B. W.; Bott, S. G. *J. Am. Chem. Soc.* **1993**, *115*, 5837.
(32) Moses, M. J.; Fettinger, J. C.; Eichhorn, B. W. *Inorg. Chem.* **2007**, *46*, 1036.
(33) Moses, M. J.; Fettinger, J. C.; Eichhorn, B. W. *Science* **2003**, *300*, 778.
(34) Knapp, C.; Zhou, B.; Denning, M. S.; Rees, N. H.; Goicoechea, J. M. *Dalton Trans.* **2010**, *39*, 426.
(35) Santandrea, R. P.; Mensing, C.; von Schnering, H. G. *Thermochim. Acta* **1986**, *98*, 301.
(36) Hooper, T. N.; Butts, C. P.; Green, M.; Haddow, M. F.; McGrady, J. E.; Russell, C. A. *Chem.—Eur. J.* **2009**, *15*, 12196.
(37) Fianchini, M.; Dai, H. X.; Dias, H. V. R. *Chem. Commun.* **2009**, 6373.
(38) Cosier, J.; Glazer, A. M. *J. Appl. Crystallogr.* **1986**, *19*, 105.
(39) Otwinowski, Z.; Minor, W. In *Processing of X-ray Diffraction Data Collected in Oscillation Mode*; Methods Enzymol.; Academic Press: New York, 1997.
(40) Sheldrick, G. M. *Acta Crystallogr.* **2008**, *A64*, 112.
(41) Betteridge, P. W.; Carruthers, J. R.; Cooper, R. I.; Prout, K.; Watkin, D. *J. Appl. Crystallogr.* **2003**, *36*, 1487.
(42) Cooper, R. I.; Thompson, A. L.; Watkin, D. J. *J. Appl. Crystallogr.* **2010**, *43*, 1100.
(43) (a) Prince, E. *Mathematical Techniques in Crystallography and Materials Science*; Springer-Verlag: New York, 1982. (b) Carruthers, J. R.; Watkin, D. J. *Acta Crystallogr.* **1979**, *A35*, 698. (c) Watkin, D. *Acta Crystallogr.* **1994**, *A50*, 411.
(44) (a) te Velde, G.; Bickelhaupt, F. M.; Baerends, E. J.; Fonseca Guerra, C.; van Gisbergen, S. J. A.; Snijders, J. G.; Ziegler, T. *J. Comput. Chem.* **2001**, *22*, 931. (b) Fonseca Guerra, C.; Snijders, J. G.; te Velde, G.; Baerends, E. J. *Theor. Chem. Acc.* **1998**, *99*, 391.(c) Baerends, E. J.; Autschbach, J.; Bashford, D.; Bérces, A.; Bickelhaupt, F. M.; Bo, C.; Boerrigter, P. M.; Cavallo, L.; Chong, D. P.; Deng, L.; Dickson, R. M.; Ellis, D. E.; van Faassen, M.; Fan, L.; Fischer, T. H.; Fonseca Guerra, C.; Ghysels, A.; Giammona, A.; van Gisbergen, S. J. A.; Götz, A. W.; Groeneveld, J. A.; Gritsenko, O. V.; Grüning, M.; Harris, F. E.; van den Hoek, P.; Jacob, C. R.; Jacobsen, H.; Jensen, L.; van Kessel, G.; Kootstra, F.; Krykunov, M. V.; van Lenthe, E.; McCormack, D. A.; Michalak, A.; Mitoraj, M.; Neugebauer, J.; Nicu, V. P.; Noodleman, L.; Osinga, V. P.; Patchkovskii, S.; Philipsen, P. H. T.; Post, D.; Pye, C. C.; Ravenek, W.; Rodríguez, J. I.; Ros, P.; Schipper, P. R. T.; Schreckenbach, G.; Seth, M.; Snijders, J. G.; Solà, M.; Swart, M.; Swerhone, D.; te Velde, G.; Vernooijs, P.; Versluis, L.; Visscher, L.; Visser, O.; Wang, F.; Wesolowski, T. A.; van Wezenbeek, E. M.; Wiesenekker, G.; Wolff, S. K.; Woo, T. K.; Yakovlev, A. L.; Ziegler, T. *ADF2009.01*; SCM, Theoretical Chemistry, Vrije Universiteit: Amsterdam, The Netherlands; http://www.scm.com.
(45) Parr, R. G.; Yang, W. *Density Functional Theory of Atoms and Molecules*; Oxford University Press: Oxford, 1989.
(46) Vosko, S. H.; Wilk, L.; Nusair, M. *Can. J. Phys.* **1980**, *58*, 1200.
(47) (a) Becke, A. D. *Phys. Rev. A.* **1988**, *38*, 3098. (b) Perdew, J. P. *Phys. Rev. B* **1986**, *33*, 8822.
(48) (a) van Lenthe, E.; Baerends, E. J.; Snijders, J. G. *J. Chem. Phys.* **1993**, *99*, 4597. (b) van Lenthe, E.; Baerends, E. J.; Snijders, J. G. *J. Chem. Phys.* **1994**, *101*, 9783. (c) van Lenthe, E.; Ehlers, A.; Baerends, E. J. *J. Chem. Phys.* **1999**, *110*, 8943.
(49) Klamt, A. *J. Phys. Chem.* **1995**, *99*, 2224.
(50) Versluis, L.; Ziegler, T. *J. Chem. Phys.* **1988**, *88*, 322.
(51) A second polymorph of sample **1** has also been observed. This species is isomorphic with **2**; however, because of poor sample crystallinity the single crystal X-ray data which were collected were of insufficient quality for the meaningful discussion of bond metric data. Cell parameters: a = 14.4314(6) Å; b = 10.7798(3) Å; c = 19.9491(9) Å; α = 90°; β = 103.2695(18)°; γ = 90°; V = 3020.6(2) Å^3. Data for this species were collected using synchrotron radiation on a CrystalLogic Kappa (3 circle) diffractometer at beamline I19 (EH1) at Diamond Light Source, Didcot.
(52) von Schnering, H. G.; Manriquez, V.; Honle, W. *Angew. Chem., Int. Ed. Engl.* **1981**, *20*, 594.
(53) Values taken from CSD version 5.30 (November 2008).
(54) Che, C.-M.; Tse, M.-C.; Chan, M. C. W.; Cheung, K.-K.; Phillips, D. L.; Leung, K.-H. *J. Am. Chem. Soc.* **2000**, *122*, 2464.
(55) (a) Chen, C. Y.; Zeng, J. Y.; Lee, H. M. *Inorg. Chim. Acta* **2007**, *360*, 21. (b) Liu, X.; Guo, G.-C.; Fu, M.-L.; Liu, X.-H.; Wang, M.-S.; Huang, J.-S. *Inorg. Chem.* **2006**, *45*, 3679. (c) Dobrzanska, L.; Raubenheimer, H. G.; Barbour, L. J. *Chem. Commun.* **2005**, 5050. (d) Mohamed, A. A.; Pérez, L. M.; Fackler, J. P., Jr. *Inorg. Chim. Acta* **2005**, *358*, 1657.
(56) Jaw, H.-R. C.; Meral Savas, M.; Rogers, R. D.; Mason, W. R. *Inorg. Chem.* **1989**, *28*, 1028.

(57) (a) Schmidbaur, H.; Scherbaum, F.; Huber, B.; Mueller, G. *Angew. Chem., Int. Ed. Engl.* **1988**, *27*, 419. (b) Scherbaum, F.; Huber, B.; Mueller, G.; Schmidbaur, H. *Angew. Chem., Int. Ed. Engl.* **1988**, *27*, 1542. (c) Scherbaum, F.; Grohmann, A.; Huber, B.; Krueger, C.; Schmidbaur, H. *Angew. Chem., Int. Ed. Engl.* **1988**, *27*, 1544.

(58) (a) Schmidbaur, H. *Chem. Soc. Rev.* **1995**, 391. (b) Pyykkö, P. *Angew. Chem., Int. Ed.* **2004**, *43*, 4412. (c) Pyykkö, P. *Chem. Rev.* **1997**, *97*, 597.

(59) Mingos, D. M. P.; Yau, J.; Menzer, S.; Williams, D. J. *J. Chem. Soc., Dalton Trans.* **1995**, 319.

NOTE ADDED AFTER ASAP PUBLICATION

This paper was published on the Web on March 22, 2011. Due to a production error, electrospray ionization mass spectrometry was incorrectly defined in the paper. The corrected version was reposted on March 30, 2011.